01,07

Formation and stabilization of dispersed „core−shell“ structures as a result of solid-phase wetting

© I.K. Razumov

Institute of Metal Physics after M.N. Mikheev, Ural Branch of Russian Academy of Sciences, Ekaterinburg, Russia

E-mail: rik@imp.uran.ru

Received July 18, 2024
Revised July 18, 2024
Accepted July 19, 2024

The use of alloying components to control the microstructure and inhibit the growth of precipitates during alloy decomposition is a promising method for developing new materials. However, in the analysis of decomposition kinetics and the mechanisms of „core−shell“ structure formation, the effect of solid-phase wetting is rarely taken into account. It is traditionally believed that wetting is more characteristic of transformations involving a liquid phase. This work demonstrates that wetting is determined by the same interatomic interaction energies responsible for decomposition, and therefore should be considered in the analysis of transformations in multi-component alloys. Furthermore, the Kinetic Monte Carlo modeling automatically takes this effect into account, while diffusion phenomenological models often neglect it. Conditions for complete and partial solid-phase wetting are formulated. The conditions for stabilizing dispersed states of the alloy in the presence of wetting are investigated.

Keywords: Ternary alloy, spinodal decomposition, dispersed states, Monte Carlo simulation, solid phase wetting.

DOI: 10.61011/PSS.2024.09.59207.197

1. Introduction

Metastable dispersed states occurred during alloys decomposition under elevated temperature with further quick cooling are of stable interest due to high operating properties of the obtained materials [1–3]. At that use of doping components is a promising method to control the structural state occurred during decomposition of the alloy [4–7]. Thus, in alloy Al-Cu high strength properties are achieved as result of formation of Guinier−Preston zones and degrade during the transformation of growing precipitates $\theta' \to \theta$ [8]. Stabilization of precipitates of phase θ' is achieved due to additions of Mn or Zr, their atoms segregate at interfaces [9,10]. In alloy αFe-Cu spinodal decomposition starts in the BCC lattice with the formation of metastable precipitates αCu [11–13], their lattice is re-arranged into FCC when size of precipitates reaches ~ 10 nm, this is accompanied by decrease in strength properties. Decelerating of growth of precipitates αCu can be ensured by additions of Ni and Al, their concentration increases at interfaces [14]. In alloy Al-Sc strength increases due to formation of precipitates Al_3Sc and decreases with their growth. Doping with Zr leads to implementation of particles of intermediate composition $Al_3Sc_xZr_{1-x}$, at that during their formation Zr forms non-equilibrium shell around the core of enriched Sc, decelerating growth of precipitates [15,16]. Thus, it is known from experiments and atomistic modeling that dispersed states arising at the intermediate stage of alloy decomposition can be stabilized by doping as a result of the formation of structures „core−shell“. But during analysis of the decomposition kinetics and mechanisms of formation of structures „core−shell“ the effect of solid-phase wetting is rarely considered. It is traditionally assumed that wetting is typical more likely for transformations involving the liquid phase.

Three main mechanisms ensuring formation of such structures were discussed. The first mechanism was suggested by Weissmuller under the theory of grain-boundary segregations [17,18]. If the impurity segregation energy at the grain boundary is higher the critical value, the equilibrium grain size occurs, it is determined by average concentration of the impurity. These concepts are easily transferred to the case of impurity segregations at interfaces with broken coherence: if the impurity segregation energy at the interface is higher the critical value, the equilibrium size of precipitates arises, depending on the average impurity concentration [19]. The phenomenon was identified by experiments in alloy Mg-Sn-Zn, where precipitates Mg_2Sn stabilize in size due to segregation of Zn atoms at interface [20]. Segregations on interfaces are observed also in alloys Al-Cu [21,22], Al-Zn-Mg [23,24], Al-Ni-Zr [25], though their stabilizing role in the decomposition is less clear in these cases.

Another mechanism of dispersed states stabilization is that primary precipitates can stimulate the formation of secondary precipitates enriched with low-mobility component in the form of a continuous or discontinuous shell, due to which the primary precipitates are isolated from the matrix and their growth rate decreases [4]. Finally, under third possible scenario the shell represents non-equilibrium near-boundary, layer of solid solution enriched with low-mobility doping component [26], formed on the intermediate stage of decomposition and dissolved (with transition to

equilibrium phases) during long-term holding. Qualitatively similar non-equilibrium shells are realized, for example, in the alloy Al-Sc-Zr [15,16]. In paper [26] the possibility was discussed of formation of non-equilibrium shells enriched with nickel around precipitates of Ag during decomposition in alloy Cu-Ag-Ni in some temperature range.

In above mechanisms of stabilization of dispersed states the absence of interaction between boundaries of precipitates (or concentration heterogeneities) of different types was supposed. In particular, in paper [4] the surface energy of precipitates A is determined by the concentration gradient $(\nabla c_{\mathrm{A}})^2$ in free energy functional, and does not depend on whether the precipitate A is in contact with matrix or with precipitate B forming the shell. However, from literature the wetting phase transition is known [27–30], which means that droplet B keeps round shape or spreads over sibstrate surface A depending whether or not the total energy of boundaries decreases as result of wetting. In model approaches such interaction of boundaries of precipitates can be considered by contribution of form $(\nabla c_{\mathrm{A}} \nabla c_{\mathrm{B}})$ in free energy functional. Previously in paper [31] during numerical solution of Chan–Hillird equations for three-component alloy we observed greater or lesser wetting of stationary particles introduced into the alloy in advance, depending on the ratio of the energy coefficients before the gradient contributions in the free energy functional. In experiments the wetting phase transition was observed for liquids on the surface of substrates [32,33], during contact of the solid phase with grain boundaries [34–38] and during the decomposition of solid films [39,40]. It looks like that experimental data on wetting phase transition on interfaces of precipitates during alloy decomposition are currently absent. In significant degree this can be associated with problem of interpretation of the experimental facts, as except wetting other factors exist (segregations on interfaces, kinetic parameters), responsible for formation of structures „core–shell" [4,19,26].

In present paper it is shown that trend of wetting is intimately connected with the potentials of interatomic interactions, in general case no suppositions are necessary for lattice distortions near the interface, and, therefore, it shall be considered during analysis of transformations in multi-component alloys. Complete or partial wetting, or its absence are implemented at different ratios of the same energy parameters that determine the decomposition thermodynamics. The conclusions are illustrated by Monte Carlo simulations of the decomposition, which automatically take into account the contribution into energy responsible for wetting. Conditions are studied of stabilization of dispersed states arising during decomposition upon complete or partial wetting.

2. Conditions of solid-phase wetting

Ginzburg–Landau (G–L) functional of free energy of binary alloy mixing has view [41,42]:

$$F = \int \left(f(c_{\mathrm{A}}) + \sigma R^2 (\nabla c_{\mathrm{A}})^2 \right) dV, \qquad (1)$$

where concentrations of components are linked by the conditions $c_A + c_B = 1$; $f(c_A, c_B)$ — density of free energy of homogeneous alloy mixing; R — small parameter of about radius of interatomic interaction, σ — energy coefficient determining surface energy. The gradient contribution in (1) describes interaction of concentration heterogeneities of component A. $\sigma > 0$ selection means energy advantage of coarsening over time of the microstructure arising during decomposition from homogeneous initial state, i.e. the presence of precipitates coalescence. Opposite situation $\sigma < 0$ is possible, for example, in microemulsions [43], colloidal suspensions and dipole liquid mixtures with Coulomb interaction [44]; in this case equilibrium droplet or lamellar structures [45,46] are formed, for their correct description additional contributions in formula (1) are required.

In case of three-component ABM-alloy the formal generalization (1) has view [47]:

$$F = \int \left(f(\{c_{\mathrm{A}}\}) + R^2 \Sigma_{\alpha,\beta} \kappa_{\alpha,\beta} (\nabla c_\alpha \nabla c_\beta) \right) dV, \qquad (2)$$

where $\alpha\beta = \{\mathrm{A}, \mathrm{B}, \mathrm{M}\}$. Using condition $c_{\mathrm{A}} + c_{\mathrm{B}} + c_{\mathrm{M}} = 1$, let's rewrite (2), excluding variable c_{M}:

$$F = \int \Big(f(\{c_{\mathrm{A}}, c_{\mathrm{B}}\}) + R^2 \times \left[\sigma_{\mathrm{A}} (\nabla c_{\mathrm{A}})^2 + \sigma_{\mathrm{B}} (\nabla c_{\mathrm{B}})^2 + \sigma_{\mathrm{AB}} (\nabla c_{\mathrm{A}} \nabla c_{\mathrm{B}}) \right] \Big) dV, \qquad (3)$$

where $\sigma_{\mathrm{A}} = \kappa_{\mathrm{AA}} + \kappa_{\mathrm{MM}} - 2\kappa_{\mathrm{AM}}$, $\sigma_{\mathrm{B}} = \kappa_{\mathrm{BB}} + \kappa_{\mathrm{MM}} - 2\kappa_{\mathrm{BM}}$, $\sigma_{\mathrm{AB}} = 2(\kappa_{\mathrm{MM}} + \kappa_{\mathrm{AB}} - \kappa_{\mathrm{AM}} - \kappa_{\mathrm{BM}})$. Coefficients $\kappa_{\mathrm{A(B)}}$ determine energy of interfaces of precipitates A(B) in matrix M, and coefficient σ_{AB} — change in surface energy during contact of precipitates A and B.

During analysis of the alloys decomposition the reasonable demand is $\sigma_{\mathrm{A(B)}} > 0$, this means absence of energy advantage of concentration gradients formation of components A or B (i.e. dispersed states) in absence of stimulus for alloy decomposition, determined by type of free energy density $f(c_{\mathrm{A}}, c_{\mathrm{B}})$. the exception is the case when impurity segregation at the interface occurs (usually as a result of violation of the lattice coherence) [19,20], then $\sigma_{\mathrm{A}} = \sigma_{\mathrm{A}}^0 - \xi c_{\mathrm{B}}$, so at ξ above the critical value the coefficient σ_{A} becomes negative, and in alloy equilibrium dispersed states can occur.

At the same time, coefficient σ_{AB} can be both above, and below zero, this is does not require any specific suppositions. $\sigma_{\mathrm{AB}} > 0$ selection means presence of partial wetting between components A and B; if σ_{AB} is higher the critical value, the full wetting phase transition can be

implemented, when one of precipitates spreads over the surface of another one [27,28].

Density of free energy of mixing in formula (2) contains contributions of enthalpy and entropy

$$f(c_A, c_B) = H_{mix} - TS_{mix}, \tag{4}$$

which can be determined under model of regular solid solution [4,48]:

$$H_{mix} = -\nu_{AB}c_Ac_B - \nu_{AM}c_Ac_M - \nu_{BM}c_Bc_M, \tag{5}$$

$$S_{mix} = -k\Sigma_\alpha c_\alpha \ln c_\alpha \tag{6}$$

where $\nu_{\alpha\beta}$ — energy of interaction of atoms of types α and β. Using condition $c_A + c_B + c_M = 1$, we can transform (5) as follows

$$H_{mix} = -\nu_{AM}c_A - \nu_{BM}c_B + \nu_{AM}c_A^2 + \nu_{BM}c_B^2 + \nu c_Ac_B, \tag{7}$$

where $\nu = \nu_{AM} + \nu_{BM} - \nu_{AB}$. Since the expressions for the fluxes of atoms are determined by the gradients of chemical potentials $\nabla(\delta F/\delta c_\alpha)$ [48], in the absence of concentration dependence of values $\nu_{\alpha\beta}$, first two terms in (7) do not contribute to fluxes and can be omitted.

Under phenomenological approach (1)–(7) coefficients $\nu_{\alpha\beta}$ and $\sigma_{A(B)}$, σ_{AB} are independent. But in fact in absence of lattice distortions values $\sigma_{A(B)}$, σ_{AB} can be expressed via the energies of interatomic interactions $\nu_{\alpha\beta}$. For this like in paper [26] let;s present the alloy energy in node $\mathbf{r}$ as

$$E(\mathbf{r}) = \Sigma_\alpha E_\alpha(\mathbf{r})c_\alpha(\mathbf{r}), \tag{8}$$

at that energy of atom of type α is determined by summation of energies of pair interaction $\phi^{\alpha\beta}(\mathbf{r})$ by nodes k of entire lattice:

$$E_\alpha(\mathbf{r}) = \Sigma_\beta\Sigma_k\phi^{\alpha\beta}(\xi_k)c_\beta(\mathbf{r} + \xi_k). \tag{9}$$

Performing in (9) expansion in terms of ξ_k, we obtain:

$$E_\alpha(\mathbf{r}) = \Sigma_\beta\Phi_{\alpha\beta}\big(c_\beta(\mathbf{r}) + R^2\Delta c_\beta(\mathbf{r})\big), \quad \Phi_{\alpha\beta} = \Sigma_k\phi^{\alpha\beta}(\xi_k). \tag{10}$$

where small parameter R characterizes effective radius of interatomic interaction, and for simplicity we assume it independent from atom type. The first term in (10) ensures determination of the mixing enthalpy

$$H_{mix} = \Sigma_{\alpha,\beta}\Phi_{\alpha\beta}c_\alpha(\mathbf{r})c_\beta(\mathbf{r}) - \Sigma_\alpha\Phi_{\alpha\alpha}c_\alpha(\mathbf{r}), \tag{11}$$

this leads to formula (5), at that interaction energies are expressed via values of pair potentials

$$\nu_{\alpha\beta} = \Phi_{\alpha\alpha} + \Phi_{\beta\beta} - 2\Phi_{\alpha\beta}, \tag{12}$$

$\nu_{\alpha\beta} < 0$ selection means presence of thermodynamic stimulus for decomposition between components α, β. Second term in (10), after substitution to (8) and integration over volume determines the gradient contribution in energy of concentration heterogeneities into G–L functional:

$$F_s = R^2\int\big(\Sigma_{\alpha,\beta}\Phi_{\alpha\beta}c_\alpha(\mathbf{r})\Delta c_\beta(\mathbf{r})\big)dV. \tag{13}$$

As it was shown in [42] using Gaussian theorema, for contributions in free energy functional the relationship is valid

$$\int\eta(c)\Delta c dV = -\int\big(\nabla\eta(c)\big)(\nabla c)dV, \tag{14}$$

where $\eta(c)$ — random function of component concentration. Then the expression (13) is converted to the form

$$F_s = -R^2\int\big[\nu_{AM}(\nabla c_A)^2 + \nu_{BM}(\nabla c_B)^2 + \nu(\nabla c_A\nabla c_B)\big]dV, \tag{15}$$

Comparing (15) and (3) we find

$$\sigma_A = -\nu_{AM}, \quad \sigma_B = -\nu_{BM}, \quad \sigma_{AB} = -\nu,$$

$$\nu = \nu_{AM} + \nu_{BM} - \nu_{AB}. \tag{16}$$

In absence of the final decomposition trend ($\nu_{\alpha\beta} > 0$) the formula (15) forecasts the non-physical result — concentration gradients increasing. Presumably, this is associated with the fact that occurred in alloy at $\nu_{\alpha\beta} > 0$ the ordering trend due to re-distribution of atoms α, β between sublattices contradicts to supposed in (9) monotonous change in concentrations upon movement from the node $\mathbf{r}$. Thus, from (15), (16) it follows that this approach is valid only in case when there is decomposition trend for all pairs of components, i. e. $\nu_{\alpha\beta} < 0$. From this the formal limitation for wetting energy appears, $\sigma_{AB} < \sigma_A + \sigma_B$.

The wetting phase transition means that precipitate B spreads over surface of precipitate A, if for interface energies the ratio is met $S_{BM} + S_{AB} < S_{AM}$ [28,35], this means that total energy of two interfaces B–M and A–B is lower than energy of single interface A–M. Link between energy of precipitate boundary and coefficient σ before the gradient contribution in G–L functional was determined in [42]. If components precipitate in pure form, and boundary width tends to zero, a rough estimate of $S_{AM} \propto \sigma_A$, $S_{BM} \sim \sigma_B$, $S_{AB} \sim \sigma_A + \sigma_B - \sigma_{AB}$ is possible. From here the condition of full wetting is $\sigma_{AB} > 2\sigma_B$, or via energy of interatomic interactions

$$\nu_{AB} > \nu_{AM} - \nu_{BM} \tag{17}$$

or

$$\nu < 2\nu_{BM}. \tag{18}$$

As in this model $\nu_{\alpha\beta} < 0$, formula (17) means that as wetted substrate only component with large energy stimulus for decomposition in matrix can be used. At this the stimulus for mutual decomposition of components A, B (forming structure „core–shell") shall be below the critical value.

Formula (16) expresses coefficients $\sigma_{A(B)}$, σ_{AB} via interaction energies $\nu_{\alpha\beta}$ in case of ideal lattice. But actually for interfaces the partial violation of lattice coherency is typical,

it contributes both to surface energies of precipitates A, B in matrix, and to their wetting energy. So, generally replacement is possible

$$\tilde{\sigma}_{\mathrm{A(B)}} = \sigma_{\mathrm{A(B)}} + \sigma^*_{\mathrm{A(B)}}, \quad \tilde{\sigma}_{\mathrm{AB}} = \sigma_{\mathrm{AB}} + \sigma^*_{\mathrm{AB}}, \tag{19}$$

where $\sigma^*_{\mathrm{A(B)}}$, σ^*_{AB} — corrections to coefficients $\sigma_{\mathrm{A(B)}}$, σ_{AB}, determined by specific nature of structure of interfaces in actual alloy. Above mentioned limitation $\sigma_{\mathrm{AB}} < \sigma_{\mathrm{A}} + \sigma_{\mathrm{B}}$, in general, should not be mandatory met for $\tilde{\sigma}_{\mathrm{A(B)}}$, $\tilde{\sigma}_{\mathrm{AB}}$.

Previously in article [4] mechanisms of formation and stabilization of dispersed state in three-component alloy were considered, including structure of type „core–shell" in supposition $\tilde{\sigma}_{\mathrm{AB}} = 0$, i. e. in absence of wetting. It turned out that even in this case, there are conditions when a shell in the form of phase of another type appears around the precipitates of one type, significantly slowing down the further growth of the precipitates. In paper [31] wetting of previously introduced in alloy fixed particles was studied. At that coefficients $\nu_{\alpha\beta}$ and $\sigma_{\mathrm{A(B)}}$, σ_{AB} under the phenomenological approach were considered as independent. In this paper we will study structures occurred during alloy decomposition from homogeneous state at different ratio of energy coefficients $\sigma_{\mathrm{A(B)}}$, σ_{AB} determined by formulas (16).

Cahn–Hilliard continual equations [41,49] with G–L functional (3) suppose smooth change in concentrations on interfaces and are not well suitable to describe thin layers of substance during wetting phase transition. Moreover, under phenomenological approach during analysis of the multi-component alloy it is difficult to determine correctly the kinetic coefficients in expressions for atom fluxes, at that equation obtained under microscopic theory are rather cumbersome [26]. So, in present paper for numerical analysis another approach is used [19], when instead of solution of continual equations of diffusion the decomposition modeling by kinetic Monte Carlo method [50].

3. Algorithm of modeling by kinetic Monte Carlo method

Let's consider 2D-model of ABM-alloy with simple square lattice. Let's $n_\alpha^{(i)} = 1$, if in node i atom of type α present, and $n_\alpha^{(i)} = 0$ in opposite case; $\Sigma_\alpha n_\alpha^{(i)} = 1$. Hamiltonian of interaction in node i, determined by occupation numbers $n_\alpha^{(i)}$ on discrete lattice, automatically considers surface contributions to energy $\sigma_{\mathrm{A(B)}}$, σ_{AB} and has view corresponding to mixing enthalpy (5):

$$H_{\mathrm{int}}^{(i)} = \sum_{i' \neq i} \left[-\nu_{\mathrm{AB}}^{(i;i')} n_A^{(i)} n_{\mathrm{B}}^{(i')} - \nu_{\mathrm{AM}}^{(i;i')} n_{\mathrm{A}}^{(i)} n_{\mathrm{M}}^{(i')} - \nu_{\mathrm{BM}}^{(i;i')} n_{\mathrm{B}}^{(i)} n_{\mathrm{M}}^{(i')} \right], \tag{20}$$

where $\nu_{\alpha\beta}^{(i;i')}$ — interaction energy of atoms of type α and β at distance determined by nodes i, i'. Let's radius of interaction of atoms is 3 coordination spheres (CS), i. e. each atom interacts with 12 neighbors; $\nu_{\alpha\beta}^{(k)}$ — interaction energy of atoms α and β on k-th sphere.

The kinetic Monte Carlo algorithm for three-component alloy is as follows [51]. A pair of neighboring atoms of different types is randomly selected. Energies of initial configuration and after re-arrangement of these atoms are calculated, E_1 and E_2. Probability of places exchange of selected atoms depends on their type, and on values of energies E_1 and E_2. It is accepted that exchange of atom with larger diffusion mobility and matrix atom is implemented with Metropolis probability: new configuration is accepted definitely, if $E_2 < E_1$; otherwise it is accepted with probability $P = \exp[(E_1 - E_2)/(k_{\mathrm{B}}T)]$. Exchange of atom with lower diffusion mobility and another atom (matrix or impurity) is implemented with Metropolis probability multiplied by ratio of amplitude frequencies of low-mobility and high-mobility components. After this the algorithm is repeated. The entropy contribution (6) in free energy is automatically considered by this procedure. For simplicity and clearness we assume that amplitude frequencies of exchange $\omega_{\alpha\beta}$ do not depend on concentrations, in particular, they are same in matrix and in bulk of precipitates of one or another type.

For easy analysis of decomposition kinetics we introduce function $\rho_\alpha(\tau)$:

$$\rho_\alpha(\tau) = \frac{S_\alpha^{(\mathrm{dec})}(\tau)}{S_\alpha^{(\mathrm{disp})}(\tau)},$$

$$S_\alpha^{(\mathrm{dec})}(\tau) = \frac{1}{K} \Sigma_i h\left(c_\alpha^{(i)}(\tau) - 0.5\right),$$

$$S_\alpha^{(\mathrm{disp})}(\tau) = \frac{a^2}{K} \Sigma_i \left(\nabla c_\alpha^{(i)}(\tau)\right)^2, \tag{22}$$

where function $S_\alpha^{(\mathrm{dec})}(\tau)$ describes evolution of degree of decomposition (portion of atoms of type α in precipitates), $S_\alpha^{(\mathrm{disp})}(\tau)$ describes degree of dispersion of precipitates (proportional to total area of their surface), $h(x)$ — Heaviside function, K — number of lattice nodes, local concentration of atoms of type α determined by formula

$$c_\alpha^{(i)} = \sum_{i' \in 3CS} \frac{n_\alpha^{(i')}}{13}.$$

From these definitions we see that function $\rho_\alpha(\tau)$ if proportional to average size of precipitate of type α, in ratio to width of interface.

Dimensionless time τ is evaluated as weighed average by re-arrangements of different types

$$\tau = \frac{\tau_{\mathrm{AB}} N_{\mathrm{AB}} + \tau_{\mathrm{AM}} N_{\mathrm{AM}} + \tau_{\mathrm{BM}} N_{\mathrm{BM}}}{N_{\mathrm{AB}} + N_{\mathrm{AM}} + N_{\mathrm{BM}}}, \tag{23}$$

where $N_{\alpha\beta}$ — number of implemented re-arrangements of atoms of types α and β, $\tau_{\alpha\beta}$ — evaluation of time by appropriate re-arrangements

$$\tau_{\alpha\beta} = \left(\sum_{k=1}^{N_{\alpha\beta}} t_{\alpha\beta}^{(k)} \right) / \left(c_\alpha^0 c_\beta^0 K^2 \right), \tag{24}$$

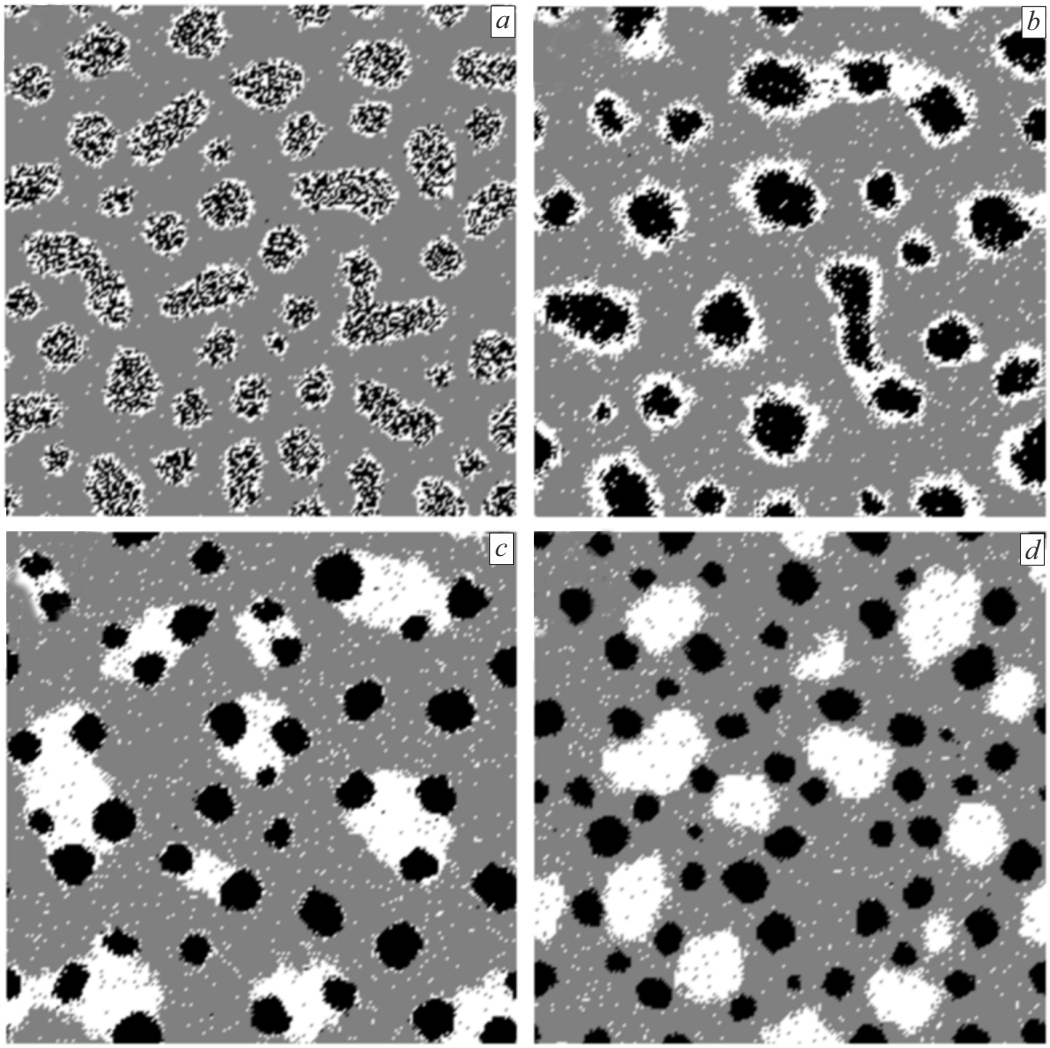

Figure 1. Characteristic decomposition patterns of three-component alloy at time corresponding to 3000 hops on average per atom of type A, $c_{\mathrm{A}}^0 = c_{\mathrm{B}}^0 = 0.2$, $\frac{\omega_{\mathrm{AB}}}{\omega_{\mathrm{AM}}} = \frac{\omega_{\mathrm{BM}}}{\omega_{\mathrm{AM}}} = 1$; $\frac{v_{\mathrm{AM}}^{(1,2,3)}}{kT} = -0.4$, $\frac{v_{\mathrm{BM}}^{(1,2,3)}}{kT} = -0.16$; $\sigma_{\mathrm{A(B)}}^* = \sigma_{\mathrm{AB}}^* = 0$; $\frac{v^{(1,2,3)}}{kT} = a)\ -0.6$, $b)\ -0.4$, $c)\ -0.24$, $d)\ 0.08$.

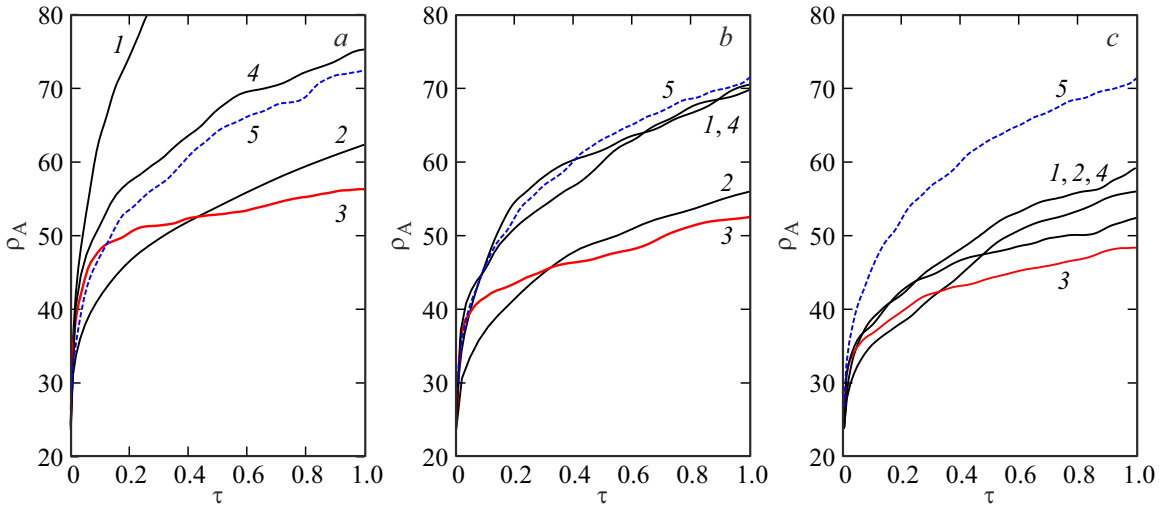

Figure 2. Evolution of function $\rho_{\mathrm{A}}(\tau)$, characterizing average size of precipitates, at $\frac{\omega_{\mathrm{AB}}}{\omega_{\mathrm{AM}}} = \frac{\omega_{\mathrm{BM}}}{\omega_{\mathrm{AM}}} = 1$ (curve *1*), 10^{-2} (curve *2*), 10^{-4} (curve *3*), 10^{-5} (curve *4*), in absence of component B (dashed curve *5*). Values of rest parameters correspond to *a*) Figure 1, *b* (complete wetting), *b*) Figure 1, *c* (partial wetting), *c*) Figure 1, *d* (absence of wetting).

where $c^0_{\alpha(\beta)}$ — average over sample concentrations of atoms of types α and β, $t^{(k)}_{\alpha\beta}$ — time corresponding to rearrangement of one pair of atoms at k-th iteration:

$$t^{(k)}_{\alpha\beta} = \left[\frac{\omega_{\alpha\beta}}{\max(\{\omega_\alpha\beta\})} P^{(k)}_{\alpha\beta}\right]^{-1}, \qquad (25)$$

where $P_{\alpha\beta}$ — Metropolis probability, $\omega_{\alpha\beta}$ — amplitude frequencies of exchange.

4. Modeling results

Let's consider the alloy in which there are stimuli for decomposition by components A and B in matrix, at that for definiteness the stimulus for decomposition for component A is higher i.e. $\nu_{AM} < \nu_{BM} < 0$. Figure 1 presents typical patterns occurred as result of such alloy decomposition upon start-up from homogeneous initial state, with different selection of energy ν, which determines wetting energy σ_{AB} (see formula (16)). Mobility of atoms of different types were selected similar. Atoms of type A hereinafter are shown in black, atoms B — white, atoms of matrix M — gray. Calculations were performed for square area with size 200×200, with periodic boundary conditions.

You can see that structure „core–shell" is implemented in range of intermediate values ν, that complies with the condition (18), at that „core" is formed from component A having larger energy stimulus for decomposition (Figure 1, *b*). Precipitates of component A grow without limit with time, so during long-time holding there is excess of component B near interface, due to this width of shell can significantly vary along the interface.

When selecting $\nu < \nu_{AM} + \nu_{BM}$ due to definition (16) energy ν_{AB} is positive, this is allowed during Monte Carlo modeling and leads to formation of precipitates of mixed composition A-B (Figure 1, *a*). When selecting $\nu > 2\nu_{BM}$ condition of complete wetting is violated (18). In this case the occurred structure depends on sign of value ν. If condition $\nu < 0$ is met, the partial wetting is implemented: at initial stages chains are formed, and then clusters of alternating precipitates of types A and B (Figure 1, *c*). If $\nu > 0$, even partial wetting has no energy advantages, therefore isolated from each other (separated by a layer of matrix phase) precipitates of types A and B are observed in the matrix (Figure 1, *d*).

Let's consider further the kinetics of formation of structure „core–shell" (corresponding to Figure 1, *b*) at different ratio of diffusion mobilities of components. Figure 2, *a* shows graphs of evolution of function $\rho_A(\tau)$, characterizing average size of precipitates (see formulas (22)–(25)) at different values of $\frac{\omega_{AB}}{\omega_{AM}}$ (curves *1*–*4*), and, for comparison, in absence of component B (dashed curve *5*). We can see that at high mobility of component B its addition to allow accelerates nucleation and growth of precipitates A (curve *1*). The decrease in the mobility of component B, down to some optimal value, leads to deceleration of the growth of precipitates A (curves *2, 3*), because the shell, enriched with the low-mobility component B, isolates precipitates A from the matrix. Thus, growth of precipitates of component A almost stop at optimal value $\frac{\omega_{AB}}{\omega_{AM}}$ (curve *3*). The further decrease in the mobility of component B is accompanied by the acceleration of the growth of precipitates A, to values close to those observed in the absence of component B (curve *4*). This occurs due to the cause that low-mobility component B is captured in volume of precipitates A during their growth.

It is interesting to note that in the absence of deceleration, the evolution of the size of precipitates A follows the usual law $\sim \sqrt{Dt}$ (D — diffusion coefficient of component A), i.e. growth rate decreases with time. Therefore, a situation is possible when at some point of time the growth rate of precipitates A becomes insufficient to capture component B into the volume of precipitates, which leads to the formation of the shell around them, which is enriched with component B, and, consequently, to sharp decrease in their growth rate. Just this situation is implemented for the curve *3*, where in section $\tau < 0.1$ the component B is captured in the volume of growing precipitates A, and at $\tau > 0.1$ around precipitates the shell is formed decelerating their growth. Thus, varying ratio $\frac{\omega_{AB}}{\omega_{AM}}$ we can change the characteristic size of precipitates, when it is reached the shell is formed stabilizing the reached state.

Figure 2, *b* presents similar calculation corresponding to situation of partial wetting (Figure 1, *c*); we can see that qualitative features of behavior of function $\rho_A(\tau)$ are kept. Finally, Figure 2, *c* presents calculation of $\rho_A(\tau)$, corresponding to absence of wetting (see Figure 1, *d*). We can see that deceleration of decomposition for component A upon addition of low-mobility component B is again implemented. In latter case at low values of $\frac{\omega_{AB}}{\omega_{AM}}$ the main cause of deceleration is the interaction of growing precipitates with impurity atoms, and at high values of $\frac{\omega_{AB}}{\omega_{AM}}$ — deceleration of coalescence in system of alternating precipitates of types A and B. Scenario of stabilization of precipitates, not requiring wetting, were considered earlier [4]. We can state that the decomposition deceleration is ensured in all cases by the optimal ratio of the mobilities of the components, whereas the wetting tendency, strictly speaking, is not a necessary condition for stabilizing the dispersed state.

Figures 3 and 4 present characteristic patterns of initial stages of decomposition under complete wetting (Figure 3) and in absence of wetting (Figure 4) at $\frac{\omega_{AB}}{\omega_{AM}} = \frac{\omega_{BM}}{\omega_{AM}} = 10^{-4}$. In both cases the decomposition starts from capturing of atoms of type B into volume of precipitates A. At more developed stage these atoms are displaced into the near-boundary region. When completely wetted, this shell is continuous, whereas in the absence of wetting it is discontinuous and tends to further breaking during the holding process. Thus, patterns of initial stages of decomposition with and without wetting at selected parameters are in some degree similar, this leads to deceleration of decomposition in both cases.

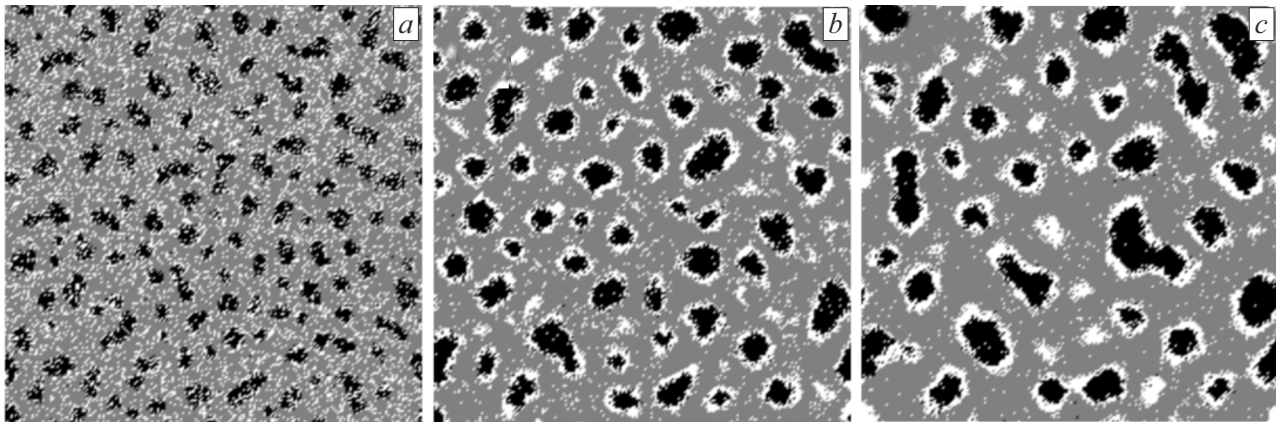

Figure 3. Kinetics of initial stages of decomposition of three-component alloy under conditions of complete wetting at $\frac{\omega_{AB}}{\omega_{AM}} = \frac{\omega_{BM}}{\omega_{AM}} = 10^{-4}$; rest parameters correspond to Figure 1, *b*. $\tau =$ *a*) 0.04, *b*) 1, *c*) 4.

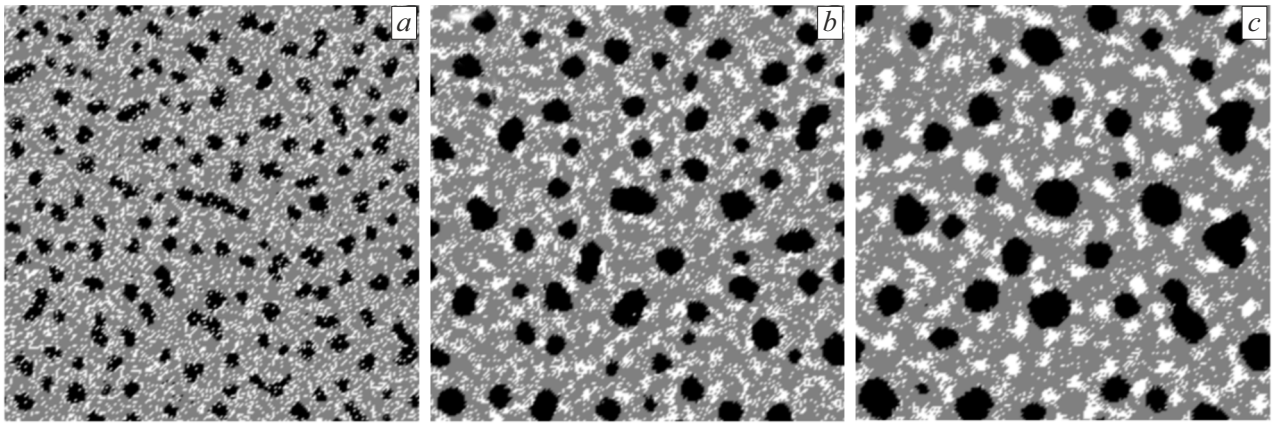

Figure 4. Kinetics of initial stages of decomposition of three-component alloy without wetting at $\frac{\omega_{AB}}{\omega_{AM}} = \frac{\omega_{BM}}{\omega_{AM}} = 10^{-4}$; rest parameters correspond to Figure 1, *d*. $\tau =$ *a*) 0.04, *b*) 1, *c*) 4.

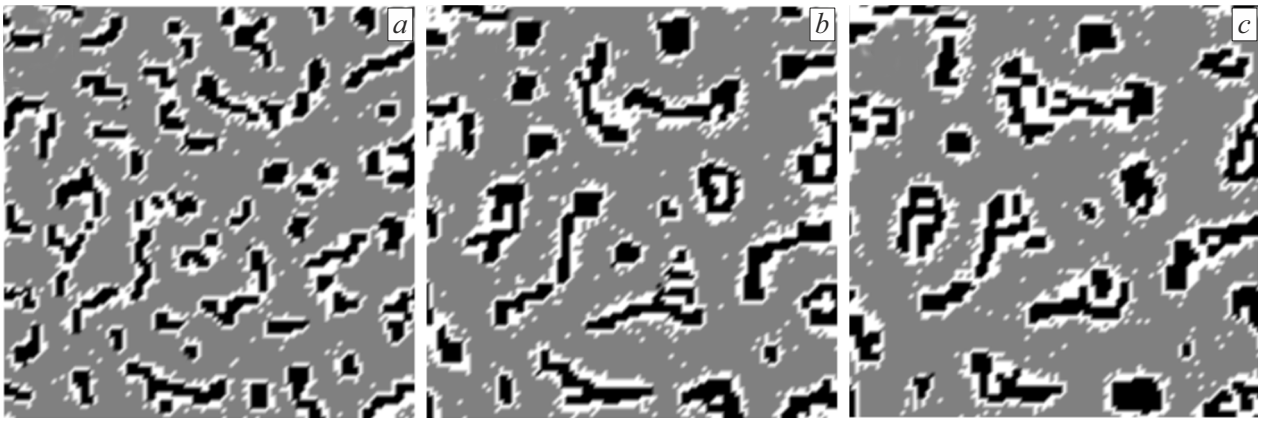

Figure 5. Kinetics of decomposition of three-component alloy under conditions of wetting at $\delta_\nu/(k_B T) = 2$; rest parameters correspond to Figure 1, *b*. $\tau =$ *a*) 0.2, *b*) 2, *c*) 4.

Finally, let's consider the case when additional contribution in the wetting energy is determined by lattice distortions near the interface (see formula (19)). Although Monte Carlo modeling is performed on ideal lattice, the additional contribution in wetting energy near the interface can be considered by replacement of $\nu \to \nu - \delta_\nu a^2 (\nabla c_A^2$, at that concentration gradient in node i is expressed via occupation number, $\nabla_x c_\alpha^{(i)} = \frac{n_\alpha(x^{(i)}+a) - n_\alpha(x^{(i)}-a)}{2a}$. Figure 5 presents the

kinetics of decomposition in situation similar to Figure 1, *b* (complete wetting), with selection of δ_ν higher some critical value, at which the surface energy of precipitates A becomes negative. To better distinguishing of small details, the size of the calculation area was reduced to 100×100. It can be seen that the morphology of the precipitates differs significantly from Figure 1, *b*: at the initial stage, component A precipitates are formed in the form of thin lamellae, surrounded by the shell of component B. During further evolution instead of coarsening the precipitates A their branching, then nucleation of colonies out of alternating lamellae A and B are implemented. This situation can be called a double-wetting phase transition, since not only component B spreads over surface A, but also component A spreads over surface B. Additional calculations show that the width of the lamellae from component A in this case increases with decrease in the average concentration of component B in the alloy.

5. Conclusion

Conditions of complete and partial wetting of precipitates during decomposition of tree-component alloy are determined. It is shown that in absence of lattice distortions the wetting energy is expressed via values of pair potentials in the lattice nodes. The kinetic Monte Carlo modeling method automatically considers this contribution to energy and allows us to study the decomposition of the alloy taking into account wetting, whereas phenomenological models using continual equations of diffusion often do not take it into account or consider the corresponding energy coefficients as independent parameters.

Kinetics of growth of precipitates of component A is studied in conditions of complete and partial wetting by component B at different ratio of diffusion mobilities of components. It is shown that shell enriched with low-mobility component B, occurring under conditions of complete wetting, can significantly decelerate the growth of precipitates A, isolating them from matrix. At that the minimum size of precipitates A is reached at optimal value of mobility of component B.

The double-wetting phase transition is predicted, which is realized if lattice distortions near the interface provoke additional contribution to the wetting energy, above a certain critical value.

Funding

The study was carried out within the framework of the State Assignment on the topic „Structure“ No. AAAA-A18-118020190116-6.

Conflict of interest

The author declares that she has no conflict of interest.

References

[1] A. Deschamps, C.R. Hutchinson. Acta Materialia **220**, 117338 (2021).
[2] Z. Xiong, I. Timokhina, E. Pereloma. Prog. Mater. Sci. **118**, 100764 (2021).
[3] S.C. Wang, M.J. Starink. Int. Mater. Rev. **50**, *4*, 193 (2005).
[4] I.K. Razumov, Yu.N. Gornostyrev. Phys. Solid State **61**, *12*, 2493 (2019).
[5] I.K. Razumov, Yu.N. Gornostyrev. FMM. V pechati (2024). (in Russian).
[6] M.D. Mulholland, D.N. Seidman. Acta Materialia **59**, *5*, 1881 (2011).
[7] P. Michaud, D. Delagnes, P. Lamesle, M.H. Mathon, C. Levaillant. Acta Materialia **55**, *14*, 4877 (2007).
[8] Yu.N. Gornostyrev, M.I. Katsnelson. Phys. Chem. Chem. Phys. **17**, *41*, 27249 (2015).
[9] A. Shyam, S. Roy, D. Shin, J.D. Poplawsky, L.F. Allard, Y. Yamamoto, J.R. Morris, B. Mazumder, J.C. Idrobo, A. Rodriguez, T.R. Watkins, J.A. Haynes. Mater Sci. Eng. A **765**, 138279 (2019).
[10] M.V. Petrik, Yu.N. Gornostyrev, P.A. Korzhavyi. Scripta Materialia **202**, 114006 (2021).
[11] M. Perez, F. Perrard, V. Massardier, X. Kleber, A. Deschamps, H. de Monestrol, P. Pareige, G. Covarel. Phil. Mag. **85**, *20*, 2197 (2005).
[12] M.E. Fine, J.Z. Liu, M.D. Asta. Mater. Sci. Eng. A **463**, *1–2*, 271 (2007).
[13] I.K. Razumov, I.G. Shmakov. Phys. Solid State **61**, *6*, 952 (2019).
[14] I.N. Kar'kin, L.E. Kar'k-na, Yu.N. Gornostyrev, A.P. Korzhavyi. Phys. Solid State **61**, *4*, 601 (2019).
[15] E. Clouet, L. Lae, T. Epicier, W. Lefebvre, M. Nastar, A. Deschamps. Nature Mater. **5**, *6*, 482 (2006).
[16] A.Yu. Stroev, O.I. Gorbatov, Yu.N. Gornostyrev, P.A. Korzhavyi. Comp. Mater. Sci. **218**, 111912 (2023).
[17] J. Weissmü ller. Nanostruct. Mater. **3**, *1–6*, 261 (1993).
[18] J.R. Trelewicz, C.A. Schuh. Phys. Rev. B **79**, *9*, 094112 (2009).
[19] I.K. Razumov. Phys. Solid State **56**, *4*, 780 (2014).
[20] C. Liu, H. Chen, J.-F. Nie. Scripta Materialia **123**, 5 (2016).
[21] L. Jiang, B. Rouxel, T. Langan, T. Dorin. Acta Materialia **206**, 116634 (2021).
[22] M.F. Chisholm, D. Shin, G. Duscher, M.P. Oxley, L.F. Allard, J.D. Poplawsky, A. Shyam. Acta Materialia **212**, 116891 (2021).
[23] B. Cheng, X. Zhao, Y. Zhang, H. Chen, I. Polmear, J.-F. Nie. Scripta Materialia **185**, 51 (2020).
[24] A.M. Cassell, J.D. Robson, X. Zhou, T. Hashimoto, M. Besel. Mater. Charact. **163**, 110232 (2020).
[25] P. Pandey, S.K. Makineni, B. Gault, K. Chattopadhyay. Acta Materialia **170**, 205 (2019).
[26] I.K. Razumov. Russ. J. Phys. Chem. A **97**, *3*, 514 (2023).
[27] J.W. Cahn. J. Chem. Phys. **66**, *8*, 3667 (1977).
[28] P.G. de Gennes. Rev. Mod. Phys. **57**, *3*, 827 (1985).
[29] A. Oron, S.H. Davis, S.G. Bankoff. Rev. Mod. Phys. **69**, *3*, 931 (1997).
[30] D. Bonn, J. Eggers, J. Indekeu, J. Meunier, E. Rolley. Rev. Mod. Phys. **81**, *2*, 739 (2009).
[31] S. Ghosh, A. Mukherjee, T.A. Abinandanan, S. Bose. Phys. Chem. Chem. Phys. **19**, *23*, 15424 (2017).

[32] J. Becker, G. Grun, R. Seemann, H. Mantz, K. Jacobs, K.R. Mecke, R. Blossey. Nature Mater. **2**, *1*, 59 (2003).
[33] X.-J. Cai, J. Genzer, R.J. Spontak. Langmuir **30**, *39*, 11689 (2014).
[34] B. Straumal, T. Lepkova, A. Korneva, G. Gerstein, O. Kogtenkova, A. Gornakova. Metals **13**, *5*, 929 (2023).
[35] B.B. Straumal. Fazovye perekhody na granitsakh zeren. Nauka, M. (2003). 327 s. (in Russian).
[36] B. Straumal, R. Valiev, O. Kogtenkova, P. Zieba, T. Czeppe, E. Bielanska, M. Faryna. Acta Materialia **56**, *20*, 6123 (2008).
[37] B.B. Straumal, O.A. Kogtenkova, A.B. Straumal, Yu.O. Kuchyeyev, B. Baretzky. J. Mater. Sci. **45**, *16*, 4271 (2010).
[38] B.B. Straumal. Fazovye perekhody na granitsakh zeren. Zhidkofaznoe i tverdofaznoe smachivanie, predsmachivanie, predplavlenie / Pod red. B.s. Bokshtejna. MISiS, M. (2004). 78 s. (in Russian).
[39] Ya.E. Geguzin, Yu.S. Kaganovsky. Diffuzionnye protsessy na poverkhnosti kristalla. Energoatomizdat, M. (1984). 128 s. (in Russian).
[40] Ya.E. Geguzin, Yu.S. Kaganovskii. Sov. Phys. Usp. **21**, *7*, 611 (1978).
[41] J.W. Cahn, J.E. Hilliard. J. Chem. Phys. **28**, *2*, 258 (1958).
[42] A.G. Khachaturyan. Teoriya fazovykh prevraschenij i struktura tverdykh rastvorov. Nauka, M. (1974). 384 s. (in Russian).
[43] G. Kaptay. Langmuir **33**, *40*, 10550 (2017).
[44] C. Sagui, R.C. Desai. Phys. Rev. Lett. **71**, *24*, 3995 (1993).
[45] G. Gonnella, E. Orlandini, J. Yeomans. Phys. Rev. Lett. **78**, *9*, 1695 (1997).
[46] G. Gonnella, E. Orlandini, J. Yeomans. Phys. Rev. E **58**, *1*, 480 (1998).
[47] D.J. Eyre. SIAM J. Appl. Math. **53**, *6*, 1686 (1993).
[48] J.W. Christian. The Theory of Transformations in Metals and Alloys. Pergamon Press (1965).
[49] L.Q. Chen. Acta Metallurgica et Materialia **42**, *10*, 3503 (1994),
[50] K. Kawasaki. In: Phase Transitions and Critical Phenomena / Eds C. Domb, M.S. Green. Academic, N.Y. (1972). V. 2. 443 p.
[51] M. Petrik, I. Razumov, Yu. Gornostyrev, I. Naschetnikova, A. Popov. Mater. **15**, *16*, 5722 (2022).

Translated by I.Mazurov